

APPARENT LIGHT REQUIREMENT FOR ACTIVATION OF PHOTOSYNTHESIS UPON REHYDRATION OF DESICCATED BEACHROCK MICROBIAL MATS¹

Ulrich Schreiber, Rolf Gademann

Julius-von-Sachs-Institut für Biowissenschaften, Universität Würzburg, Julius-von-Sachs Platz 2, D-97082 Würzburg, Germany

Paul Bird

Centre of Marine Studies, University of Queensland, St. Lucia, 4072 Queensland, Australia

Peter J. Ralph

Multiscale Ecosystem Unit, University of Technology Sydney, Gore Hill, NSW, Australia

Anthony W. D. Larkum

School of Biological Sciences, University of Sydney, NSW 2006, Australia

and

Michael Kühl²

Marine Biological Laboratory, University of Copenhagen, Strandpromenaden 5, DK-3000 Helsingør, Denmark

Photosynthetic electron transport of beachrock microbial mats growing in the intertidal zone of Heron Island (Great Barrier Reef, Australia) was investigated with a pulse amplitude modulation chl fluorometer providing four different excitation wavelengths for preferential excitation of the major algal groups (cyanobacteria, green algae, diatoms/dinoflagellates). A new type of fiberoptic emitter-detector unit (PHYTO-EDF) was used to measure chl fluorescence at the sample surface. Fluorescence signals mainly originated from cyanobacteria, which could be almost selectively assessed by 640-nm excitation. Even after desiccation for long time periods under full sunlight, beachrock showed rapid recovery of photosynthesis after rehydration in the light ($t_{1/2} \sim 15$ min). However, when rehydrated in the dark, the quantum yield of energy conversion of PSII remained zero over extended periods of time. Parallel measurements of O₂ concentration with an oxygen microoptode revealed zero oxygen concentration in the surface layer of rehydrated beachrock in the dark. Upon illumination, O₂ concentration increased in parallel with PSII quantum yield and decreased again to zero in the dark. It is proposed that oxygen is required for preventing complete dark reduction of the PSII acceptor pools via the NADPH-dehydrogenase/chlororespiration pathway. This hypothesis is supported by the observation that PSII quantum yield could be partially induced in the dark by flushing with molecular oxygen.

Key index words: beachrock; cyanobacteria; photosynthesis; oxygen; chl fluorescence; microsensor; state 1/state 2

Abbreviations: EDF, emitter-detector unit; F_o, fluorescence yield of dark-adapted sample; F_m, maximal fluorescence yield measured during saturation pulse; F_v, variable fluorescence yield; LED, light-emitting diode; PAM, pulse amplitude modulation; PQ, plastoquinone

Beachrock consists of carbonate-cemented rock of varying composition occurring in the upper tidal zone of many subtropical and tropical marine environments. Beachrock is colonized by a variety of microorganisms with a predominance of epilithic, chasmolithic, and endolithic cyanobacteria, which can form a dense microbial mat at the beachrock surface. Although geological and geochemical studies of beachrock are relatively abundant in the literature, very little is known about the biology and biogeochemistry of beachrock. Biological studies have mostly focused on faunistic and floristic accounts (e.g. Cribb 1966, Brattström 1992) and of the possible role of microorganisms in the formation of beachrock (e.g. Neumeier 1999, Webb et al. 1999). To our knowledge, the comprehensive study of Krumbein (1979) represents the most detailed account of beachrock biogeochemistry, and very little is known about the ecophysiology of microbial communities in beachrock.

The beachrock on Heron Island, Great Barrier Reef consists of microbialites and micritic aragonite cement, the formation of which is induced by biological activity (Davies and Kinsey 1973, Webb et al. 1999). Three characteristic types of beachrock have been identified (Stephenson and Searles 1960, Cribb 1966): a dark brownish-black colored zone in the upper littoral, a pale whitish-pink zone in the intermediate tidal zone, and a pale greenish-white zone extending across the low tide mark. The different zones are

¹Received 8 June 2001. Accepted 2 November 2001.

²Author for correspondence: e-mail mkühl@zi.ku.dk.

characterized by a different composition of cyanobacteria and microalgae (see Cribb 1966).

A prominent feature of beachrock is periodical dessication and exposure to extreme irradiance. In this study we investigated the photosynthesis of microbial mats covering the uppermost brownish-black zone, which is most prone to dessication and irradiance stress. The goal of the present study was to investigate physiological mechanisms involved in the recovery of photosynthesis of beachrock cyanobacteria when rehydrated after a period of desiccation. The photosynthesis of intact beachrock microbial mats was analysed by noninvasive pulse amplitude modulated (PAM) chl fluorescence measurements (Schreiber et al. 1986) in combination with fiberoptic oxygen microsensors (Klimant et al. 1995). Both techniques are used increasingly in aquatic photosynthesis studies (e.g. Kühl et al. 2001) and are applied here to epilithic cyanobacterial communities of beachrock for the first time.

Chl fluorescence provides detailed information on photosynthetic reactions (Krause and Weis 1991, Schreiber et al. 1994). In particular, PAM fluorescence measurements allow the assessment of the effective quantum yield of energy conversion at PSII reaction centers with the help of short pulses of saturating light (so-called saturation pulses) (Schreiber et al. 1986, 1994, Genty et al. 1989). Fluorescence yield is controlled by two major types of quenching mechanisms. One mechanism is photochemical quenching by charge separation at PSII, which is maximal when all reaction centers are open (i.e. all primary acceptors are oxidized) and minimal when all centers are closed (i.e. all primary acceptors are reduced). Thus, at maximal photochemical quenching the minimal fluorescence yield (F_0) is observed, whereas at minimal photochemical quenching the maximal fluorescence yield (F_m) is observed. Another mechanism is non-photochemical quenching, which controls fluorescence yield at the pigment level independently of the openness of the reaction centers. Hence, nonphotochemical quenching also affects the F_m level, which can be selectively assessed by a saturation pulse, which transiently closes all reaction centers.

Nonphotochemical quenching can reflect various processes that withdraw excitation energy from PSII, including the controlled dissipation of excess energy into heat (so-called energy-dependent quenching) (Krause et al. 1982, Demmig-Adams and Adams 1992) and the regulated transfer of energy from PSII to PSI, associated with the so-called pigment state 2 (Bonaventura and Myers 1969, Williams and Allen 1987, Quick and Stitt 1989, Allen 1992). The latter aspect is particularly important for the interpretation of chl fluorescence changes in cyanobacteria (Allen 1992, Schreiber et al. 1995), which constitute the dominant component of the beachrock microbial mats investigated in the present study. In cyanobacteria the major antenna pigments of PSI (chl *a*) and PSII (phycobilins) display markedly different excitation spectra, and the regulatory mechanism of pigment state shifts is

particularly important to ensure a balanced excitation of the two photosystems. State 2 is induced when a high reduction level of the plastoquinone (PQ) pool is reached for a significant period of time (several minutes). As a consequence of the shift to state 2, photon capture by PSII is down-regulated with respect to PSI and the PQ pool is oxidized. Conversely, a shift to state 1 is induced when the PQ pool is oxidized in the light due to preferential PSI excitation (Allen 1992). In cyanobacteria, the light-induced state 2–state 1 shift is relatively fast ($t_{1/2} < 1$ min) (Schreiber et al. 1995).

In the present investigation of beachrock, a new type of fiberoptic chl fluorometer PHYTO-PAM EDF (Heinz Walz GmbH, Effeltrich, Germany) was applied, which was specifically developed (by the first author of the present report) for the study of microphytobenthos, periphyton, and microbial mats with heterogeneous populations of photosynthetically active organisms. With this new device, chl fluorescence is excited simultaneously at four different wavelengths, thus providing coarse excitation spectra that contain information on the contribution of various types of pigmented organisms to the overall fluorescence signal (Kolbowski and Schreiber 1995, Schreiber 1998).

MATERIALS AND METHODS

Beachrock samples. Beachrock was collected from the upper brownish-black zone at the southern shore of Heron Island (152° 6' E, 20° 29' S). (See Webb et al. [1999] for a detailed description and pictures of the sampling site.) The beachrock was covered by an ~1- to 1.5-mm-thick microbial mat with a dense crumbly structure, which was predominantly composed of cyanobacteria (mainly *Entophysalis* sp., *Calothrix* sp., and *Lyngbya* sp.). An ~30-mm-thick slab of the surface was separated from a larger rock with the help of a seawater-cooled diamond-tipped circular saw, from which replicate samples of approximately 25 × 25 × 30 mm were cut. The samples were kept outdoors in a bath of continuously renewed seawater in natural daylight (up to ~2500 $\mu\text{mol quanta}\cdot\text{m}^{-2}\cdot\text{s}^{-1}$) for several hours every day and were exposed to dry air for the rest of the time. Experiments were carried out with samples desiccated for at least 8 h. For measurements, the samples were transferred to a darkened dish that could be filled with filtered aerated seawater covering the sample. In some experiments the seawater was flushed for 15 min with pure oxygen or nitrogen before addition to the samples.

Chl fluorescence measurements. Chl fluorescence was measured with a PHYTO-PAM chl fluorometer (commercially available from Heinz Walz GmbH, Effeltrich, Germany) equipped with a special emitter-detector unit (PHYTO-EDF) designed for the investigation of microphytobenthos, periphyton, and microbial mats. The PHYTO-EDF features polyfurcated fiberoptics connected to various measuring and actinic light-emitting diode (LED) light sources via miniature fiber couplers and to a photomultiplier detector. Single 1-mm plastic fibers were coupled to 470, 525, 640, and 665 nm measuring light LEDs, whereas four 1-mm fiber branches were coupled to actinic LEDs (peak 660 nm). A single 1.5-mm plastic fiber carried the fluorescence signal to the detector, which was protected by a long-pass filter ($\lambda > 700$ nm). The combined fiberoptics had a 4-mm active diameter at their joint end. A perspex cylinder (50 mm long and 4 mm in diameter) served for randomization of the various light beams. Measurements were carried out with a distance of ~2 mm between the tip of the perspex cylinder and the surface of the beachrock sample.

Ambient light was prevented from reaching the sample with the help of a darkening hood. The minimal measuring light

frequency was applied, corresponding to an integrated intensity of $0.15 \mu\text{mol quanta}\cdot\text{m}^{-2}\cdot\text{s}^{-1}$ PAR, the actinic effect of which could be neglected. The measuring light intensity of the different wavelengths was similar. When actinic illumination was applied, this amounted to $120 \mu\text{mol quanta}\cdot\text{m}^{-2}\cdot\text{s}^{-1}$ of 660 nm light. Full *in situ* irradiance of the beachrock amounted to $\sim 2500 \mu\text{mol photons}\cdot\text{m}^{-2}\cdot\text{s}^{-1}$, and the actinic light did not lead to any photoinhibition. During actinic illumination and application of saturation pulses, the measuring frequency was automatically increased by a factor of 128 to improve the signal-to-noise ratio and time resolution. Saturation pulses were applied with the actinic light LEDs (660 nm). Saturation pulses had an intensity of $\sim 1800 \mu\text{mol quanta}\cdot\text{m}^{-2}\cdot\text{s}^{-1}$, which proved enough for full PSII closure.

The PHYTO-PAM was operated in conjunction with a notebook PC and the PhytoWin data acquisition software (Heinz Walz GmbH) provided with the instrument. In applications with phytoplankton samples, a major purpose of this system is the deconvolution of fluorescence responses of the major algal groups. In the case of beachrock, this aspect was of minor importance, because the signal was dominated by cyanobacterial fluorescence. Hence, the presented data were mostly derived from signals obtained with the 640-nm measuring light, where maximal responses were obtained. In the few experiments where fluorescence signals were deconvoluted, "reference spectra" of the following organisms were used: *Synechococcus* sp. (blue), *Ankistrodesmus braunii* (green), and *Phaeodactylum tricornutum* (brown). The reference spectra were recorded in suspensions with a high chl contents ($\sim 10 \mu\text{g chl}\cdot\text{mL}^{-1}$) to approach the state of the highly pigmented organisms in microbial mats.

The PHYTO-PAM monitors continuously the chl fluorescence yield (F) using four different excitation wavelengths simultaneously. Hence, there are four independent primary signals, F_{470} , F_{525} , F_{640} , and F_{665} . In the absence of actinic light, these signals correspond to F_0 , the fluorescence yield of a dark-adapted sample, because the integrated intensity of the measuring light does not induce the accumulation of reduced PSII electron acceptors. Each actual "measurement" by the PHYTO-PAM (the data being saved in a "report file") involves the application of a saturation pulse to determine the maximum fluorescence yield (F_m) and thus the increase of fluorescence yield induced by the saturation pulse (ΔF , denoted as dF by the PhytoWin software). Briefly, before the saturation pulse, the momentary fluorescence yield ($F = F_t$) is measured, which may correspond to F_0 if the sample is dark adapted or any other fluorescence yield between F_0 and F_m if the sample is illuminated. In any case, a ΔF is measured that when related to the maximal fluorescence yield in the momentary state of the sample gives a reliable measure of the quantum yield of energy conversion of PSII: $Y = \Delta F/F_m$ (Genty et al. 1989). Formally, with a dark-adapted sample, $\Delta F/F_m$ corresponds to F_v/F_m , a frequently used parameter for the assessment of the maximal quantum conversion efficiency of PSII. However, although this parameter is well defined and readily accessible in the study of green plants, this is not the case with cyanobacteria, which are mainly dealt with in the present study.

In contrast to green plants, the dark-adapted state in cyanobacteria is not characterized by maximal photochemical and minimal nonphotochemical quenching (see e.g. Schreiber et al. 1995). Therefore, when dealing with cyanobacteria, the use of conventional F_v and F_v/F_m parameters (defined in van Kooten and Snel 1990) are problematic. It does not make sense to distinguish between F_m (maximal fluorescence yield in the dark-adapted state) and F_m' (maximal fluorescence yield in the illuminated state) because the "true F_m " is not well defined. Consequently, and for the sake of simplicity, in the present report all maximal fluorescence yields determined with the help of a saturation pulse are denoted as F_m . Likewise, all fluorescence yields measured shortly before a saturation pulse are denoted as F . If not stated otherwise, the data presented in this communication correspond to F , F_m , ΔF , and Y as measured with 640-nm excitation, which is absorbed preferentially by phycoobilins in cyanobacteria.

Measurements of oxygen concentration. Oxygen concentration was measured with an oxygen microoptode (Klimant et al. 1995; Sensor type B, Presense GmbH, Germany) coupled to a portable fluorescence lifetime measuring system (Microx TX, Presense GmbH, Germany). The system was connected to a PC via a serial interface. Calibration of the microoptode signal and data acquisition was controlled by the supplied software for the instrument. The oxygen microoptode was connected to the instrument via a standard ST-fiber connector, and a two-point calibration was performed at experimental temperature and salinity by recording the sensor signal in fully aerated seawater and in seawater made anoxic by addition of sodium dithionite. The response time of the microoptode was ~ 5 s. For measurements on the beachrock, the microoptode was mounted in a manually operated micromanipulator (MM33, Märtzhäuser GmbH, Germany) and the measuring tip was carefully positioned onto the surface of the beachrock at an insertion angle, which still allowed the perspex rod of the PHYTO-PAM EDF fiber to keep a distance of ~ 2 mm relative to the surface (see also above). The sample surface was covered with seawater, so that the tip of the microoptode and the end of the perspex rod were immersed.

RESULTS

Basic information provided by the PHYTO-PAM. Figure 1 shows the fluorescence responses of a beachrock sample after rehydration in natural sunlight, as displayed on the PC monitor screen by the PhytoWin software. The fluorescence yields, measured simultaneously with 470-, 525-, 640-, and 665-nm excitation, are displayed numerically and graphically (bars). Although the signal excited at 640 nm was distinctly higher than that at 665 nm, relatively low signals were observed with 470- and 525-nm excitation. This excitation pattern is typical for cyanobacteria, where phyco-cyanin and allophycocyanin (strong absorption at 620–640 nm) constitute the major accessory antenna pigments transferring energy to chl *a* in PSII. The values of the parameter F , as well as the corresponding bars, represent the momentary fluorescence yields. Upon application of a saturation pulse, first the momentary fluorescence yield (F) and briefly afterward the maximal fluorescence yield (F_m) are sampled. The PhytoWin software saves the momentary fluorescence yield under F_t and the saturation pulse induced increase of fluorescence yield ($\Delta F = F_m - F_t$) under dF . Due to the high signal-to-noise ratio in the given application, the values of F_t and F are identical; therefore, for the sake of simplicity the momentary fluorescence yield will be generally denoted by F in the present study (see also Materials and Methods). The yield parameter is derived from the expression $dF/(F + dF)$, which corresponds to the commonly known expressions F_v/F_m or $\Delta F/F_m$ for the effective quantum yield of energy conversion in PSII (Genty et al. 1989, Schreiber et al. 1994) (for nomenclature see Materials and Methods). The relatively low apparent quantum yield of 0.37 at 640-nm excitation is typical for cyanobacteria (Schreiber et al. 1995). The somewhat higher value at 665-nm excitation indicates an additional, albeit low, fluorescence contribution of green algae, which absorb strongly at that wavelength and displays higher values of variable fluorescence.

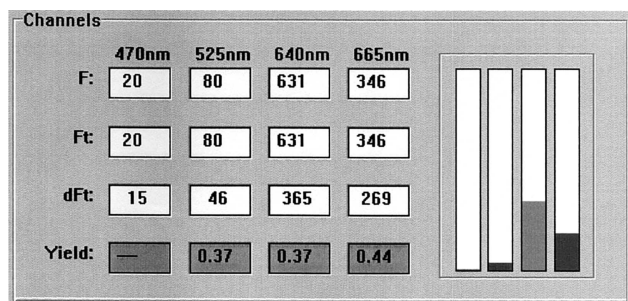


FIG. 1. Fluorescence responses of a beachrock sample after rehydration in natural sunlight and 5 min dark adaptation. The Channel screen of the PhytoWin user interface is depicted. A saturation pulse was applied to assess the effective quantum yield of PSII (yield parameter) via the induced fluorescence increase (dF). F_i is the fluorescence yield briefly before the saturation pulse. $F_i + dF_i$ corresponds to the maximal fluorescence yield reached during the saturation pulse, F_m . The bar diagram shows the momentary fluorescence yields, F , with 470-, 525-, 640-, and 665-nm excitation (from left to right), respectively.

Figure 2 shows the result of the deconvolution routine. The data indicate that about 9/10 of the fluorescence measured from the top layer of the investigated beachrock was originating from cyanobacteria, whereas the remaining 1/10 was due to green algae. Microscopic observations revealed the presence of small quantities of *Enteromorpha intestinalis*; no diatoms or dinoflagellates could be detected either in the deconvoluted fluorescence data or by microscopic observations. Although the apparent quantum yield of the green algae was almost twice that of the cyanobacteria, their contribution to the 640-nm signal was negligible, as suggested by the almost identical yield values for cyanobacteria (yield = 0.35 for “blue”) and 640-

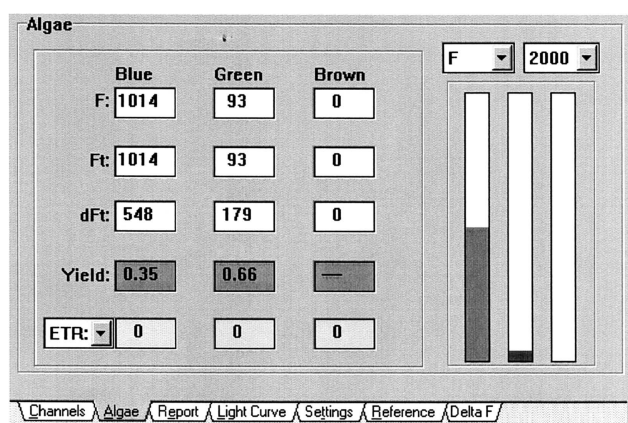


FIG. 2. Deconvoluted fluorescence data of a beachrock sample rehydrated in natural sunlight, as displayed on the Algae screen of the PhytoWin user interface. The bar diagram shows the deconvoluted momentary fluorescence yields, F , of cyanobacteria (blue), green algae (green), and diatoms and dinoflagellates (brown) (from left to right), respectively. The corresponding original data are presented in Fig. 1. For further explanations, see legend to Fig. 1 and text.

nm excitation (yield = 0.37). The overall signal was thus dominated by cyanobacteria, particularly when measured with 640-nm excitation. Therefore, in the following experiments on rehydration of beachrock and on the apparent light activation of photosynthetic electron transport, we focused on the original fluorescence parameters measured with 640-nm excitation.

Fluorescence changes upon rehydration. In Fig. 3 the fluorescence changes upon rehydration of beachrock are presented, as measured with 640-nm excitation and repetitive application of saturation pulses at 60-s intervals for assessment of variable fluorescence yield. Desiccated beachrock exhibited a rather low fluorescence yield, which upon addition of seawater rapidly increased by a factor of ~ 6 ($t_{1/2} \sim 1$ min) before it declined more slowly to an intermediate level ($t_{1/2} \sim 2$ min). No variable fluorescence could be induced by saturation pulses neither in the desiccated state nor after rehydration in the dark (Fig. 3A). However, when rehydration took place in the presence of continuous actinic light (Fig. 3B), variable fluorescence (i.e. a difference between F and F_m) was slowly induced, thus reflecting the recovery of PSII activity.

Light-induced changes of fluorescence and effective quantum yield. When rehydrated beachrock samples were kept in the dark, no variable fluorescence could be induced by saturation pulses over extended periods of time (from minutes to hours), thus indicating a per-

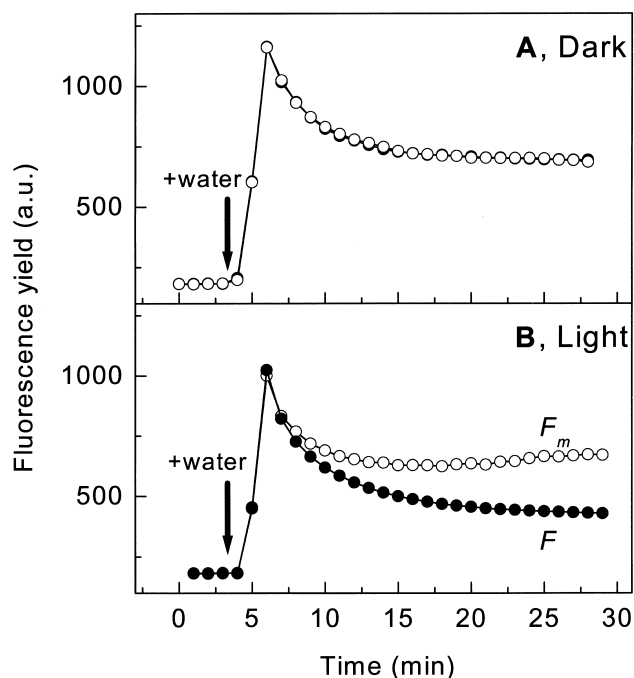


FIG. 3. Time-dependent changes of fluorescence yield upon rehydration of desiccated beachrock samples. (A) Rehydration of sample kept in the dark, except for the weak measuring light. (B) Rehydration of sample illuminated with $120 \mu\text{mol quanta} \cdot \text{m}^{-2} \cdot \text{s}^{-1}$ of 660-nm actinic light. Aerated filtered seawater was added where indicated and covered the complete sample. Saturation pulses were applied repetitively at 1-min intervals to assess variable fluorescence.

sistent blockage of PSII activity (Fig. 3A). When rehydration occurred in the light, variable fluorescence developed after about 5 min and reached a maximum after about 25 min (Fig. 3B). To elucidate the underlying mechanisms of inhibition and recovery, the dark–light–dark induction kinetics of fluorescence were investigated. Figure 4A shows the fluorescence responses of a beachrock sample, which had been rehydrated in the dark for 20 min. After this time, changes in fluorescence caused by the hydration process were largely terminated (see Fig. 3A), but no variable fluorescence was observable (i.e. the values of F and F_m were identical). Immediately after onset of actinic illumination, variable fluorescence developed, thus indicating the recovery of photosynthetic activity. The light-on response of the fluorescence yield (F) consisted of a small rise followed by a large decline. In the light-on response of F_m , the initial rise was more pronounced, whereas the subsequent decline did not fall much below the initial dark level. At light-off, both signals displayed a rapid drop. In the following dark period, the F value showed a large amplitude slow rise, whereas F_m remained almost unchanged.

In Fig. 4B the corresponding changes of the effective PSII quantum yield are shown. In the given example, the deconvoluted quantum yields for the cyanobacteria (Y_{blue}) and green algae (Y_{green}) are displayed

as well as those determined with 640-nm excitation (Y_{640}), which were derived from the original fluorescence data in Fig. 4A. Comparison of the light-induced Y_{640} and Y_{blue} responses confirmed that the cyanobacterial signal was well described by the 640-nm signal. However, it was also apparent that the Y_{green} response differed from the Y_{blue} response, as it increased distinctly faster ($t_{1/2} < 1$ min as compared with $t_{1/2} \sim 15$ min) and reached a substantially higher level (0.55 as compared with 0.27). After light-off, both quantum yields showed a transitory increase, as may be expected upon dark reoxidation of the intersystem electron transport chain. Thereafter, both quantum yields declined with similar kinetics ($t_{1/2} \sim 20$ min). It can be seen that the slow decline matched the slow rise of the fluorescence yield (F) (Fig. 4A).

Green algae are generally known to display higher values of $Y = \Delta F/F_m$ than cyanobacteria, which is in line with the results presented in Fig. 4B. Hence, it appears likely that the Y_{green} response indeed reflects a population of green algae in the microbial mat. However, because this population was very small as compared with the dominating cyanobacteria, we concentrated our efforts on the cyanobacteria, for assessment of which deconvolution was not required. Therefore, in the following experiments only the responses with 640-nm excitation are presented, which closely follow the responses of the dominating cyanobacteria (compare Y_{640} and Y_{blue} in Fig. 4B).

The dark–light–dark induction kinetics of rehydrated beachrock displayed in Fig. 4 differs considerably from corresponding kinetics known for higher plants or for cyanobacteria and green algae in suspension. Normally, the fluorescence yield of a dark-adapted sample is minimal and dark–light induction involves a rapid rise of fluorescence yield to a high level, followed by a slow decline to a lower stationary yield. This transition is also known as the Kautsky effect (Kautsky and Hirsch 1931). The observed induction kinetics of beachrock are reminiscent of that described for *Scenedesmus obliquus* under conditions of extreme anaerobiosis after prolonged dark adaptation (Schreiber and Vidaver 1974, 1975). This earlier work suggested that a hydrogenase is activated under anaerobic conditions, which causes slow reduction of the intersystem electron transport chain in the dark, accompanied by a rise in fluorescence yield from a minimal level, F_o , to a maximal level, F_m . We hypothesized that after rehydration in the dark, the beachrock microbial mat became anaerobic due to respiratory activity in combination with a slow rate of O_2 diffusion across the diffusive boundary layer overlaying the wetted beachrock. The role of oxygen was now investigated using an O_2 microelectrode in combination with the PAM fiber optics sensor.

Parallel measurements of O_2 concentration and chl fluorescence. To test the working hypothesis that photosynthesis of dark-rehydrated beachrock is blocked due to anaerobiosis, parallel measurements of O_2 concentration and chl fluorescence were carried out. O_2

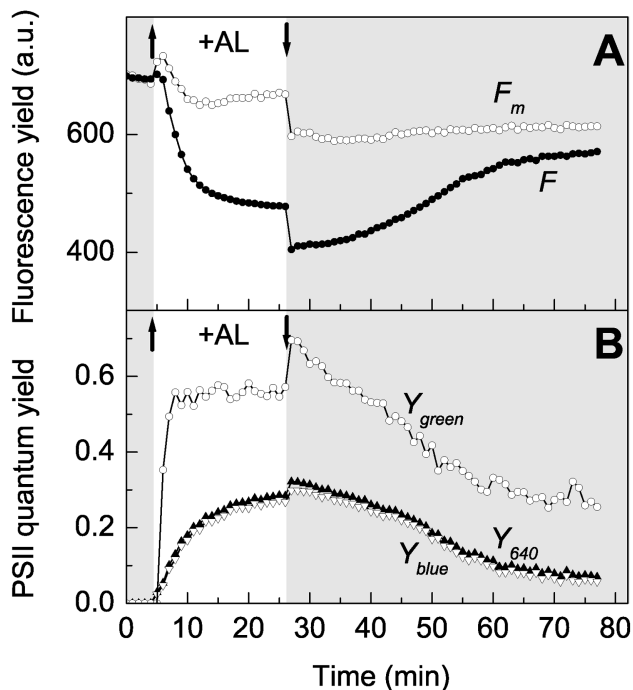


FIG. 4. Dark–light–dark induction transients of beach rock sample previously rehydrated in the dark. (A) Induction transients of fluorescence yield. (B) Induction transients of the effective PSII quantum yield measured with 640-nm excitation (Y_{640}) in comparison with the deconvoluted effective PSII quantum yields in cyanobacteria (Y_{blue}) and green algae (Y_{green}). For other conditions, see legend to Fig. 1. AL, actinic light ($120 \mu\text{mol photons}\cdot\text{m}^{-2}\cdot\text{s}^{-1}$).

concentration was assessed with an oxygen microoptode that allows local measurements in the surface layer of the sample without disturbing the O_2 concentration gradient. The presence of a diffusive boundary layer limiting O_2 exchange between beachrock and overlaying water was confirmed in a detailed microsensor study, published separately. Figure 5 shows the dynamics of oxygen and fluorescence of a beachrock sample, which was rehydrated for ca. 10 min in the dark before the onset of illumination. After illumination, the sample was kept in the dark for ~ 10 min before onset of the second illumination period, which was again followed by a dark period.

In the initial dark phase after rehydration, no variable fluorescence could be induced by saturation pulses, and the O_2 concentration at the beachrock surface was zero. After onset of illumination, O_2 concentration increased continuously, in parallel with an increase of the variable fluorescence and of the effective PSII quantum yield. Upon darkening there was a rapid O_2 uptake with O_2 concentration reaching the zero level within less than 5 min ($t_{1/2} \sim 1$ min). At the same time, complex changes of F and F_m were observed, with F showing a rapid drop followed by a slower rise and F_m showing a biphasic decline interrupted by a transient peak. These fluorescence changes translate into a rapid rise and consequent decline of PSII quantum yield ($\Delta F/F_m$) after onset of darkness. However, PSII quantum yield did not decline to the zero level, in contrast to the O_2 concentration, suggesting that a strict O_2 requirement for induction of photosynthetic electron transport may apply only after prolonged dark adaptation. This was also indicated by the observation that both the O_2 concentration and the PSII quantum yield, as well as the F and F_m values, increased much faster after onset of the second illumination period. When the sample was darkened again after the second illumination period, similar responses of oxygen concentration and the fluorescence parameters were observed as after the first illumination period. Although both O_2 concentration and PSII quantum yield declined in the dark, complete O_2 deficiency within the beachrock was not directly correlated with complete suppression of PSII quantum yield. The quantum yield did, however, decline slowly over extended periods of darkness.

Rehydration of dark-adapted beachrock in presence and absence of O_2 . The data presented in Fig. 5 give clear evidence that in rehydrated beachrock low quantum yields of photosynthetic energy conversion coincide with low O_2 concentration; when a dark-adapted rehydrated sample was illuminated, O_2 concentration and PSII quantum yield increased in parallel. The question remained whether there is a strict light requirement or whether O_2 as such can open PSII reaction centers in the dark. This question was addressed in an experiment that compared the fluorescence responses of dark-adapted beach-rock samples rehydrated in seawater flushed with either O_2 or N_2 (Fig. 6). In both cases the PSII quantum yield remained

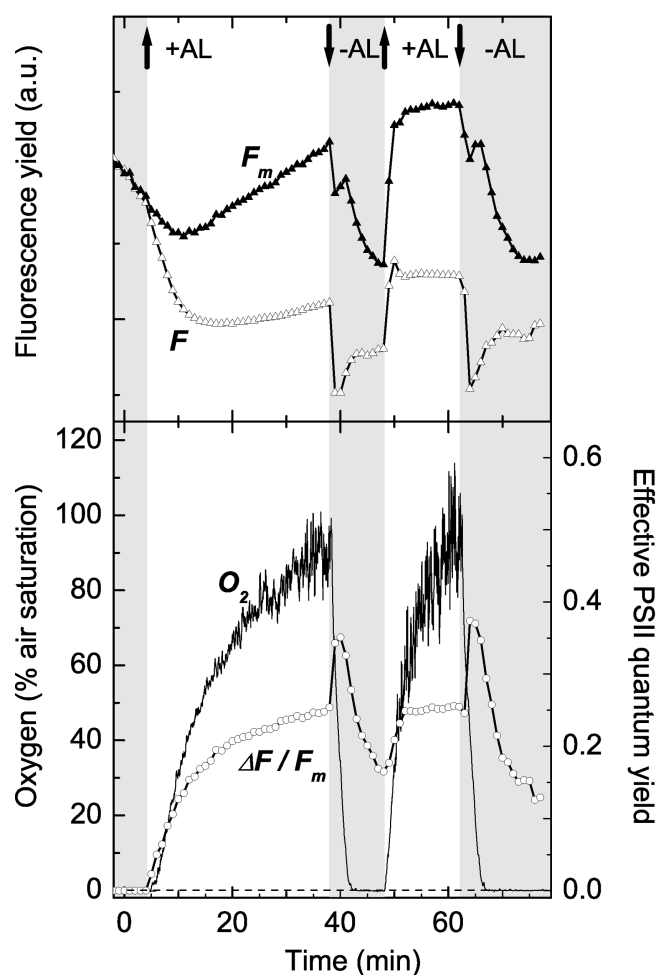


FIG. 5. Simultaneous recordings of chl fluorescence and oxygen concentration during two consecutive dark-light-dark transitions of a beachrock sample rehydrated in the dark. Oxygen concentration was measured at the beachrock surface with an oxygen microoptode (see Materials and Methods). Actinic light (AL) was switched on/off where indicated. Fluorescence was excited at 640 nm, and the depicted effective PSII quantum yield, $\Delta F/F_m$, corresponds to the Y_{640} parameter.

zero during the first 5 min after rehydration in darkness, similarly to a sample rehydrated in the light (see Fig. 3B). However, after the first 5 min, there was a small rise of PSII quantum yield only in the O_2 flushed sample. Furthermore, the presence of O_2 enhanced the rate of the light-induced increase of PSII quantum yield, whereas the decline of quantum yield upon redarkening was suppressed. Hence, our data suggest that O_2 can stimulate quantum yield both in dark-adapted and illuminated samples.

DISCUSSION

The present investigation was initiated by the observation that desiccated beachrock samples after being rehydrated in the dark showed a total lack of variable fluorescence. We interpreted this as a blockage of energy conversion in PSII. PAM fluorescence measure-

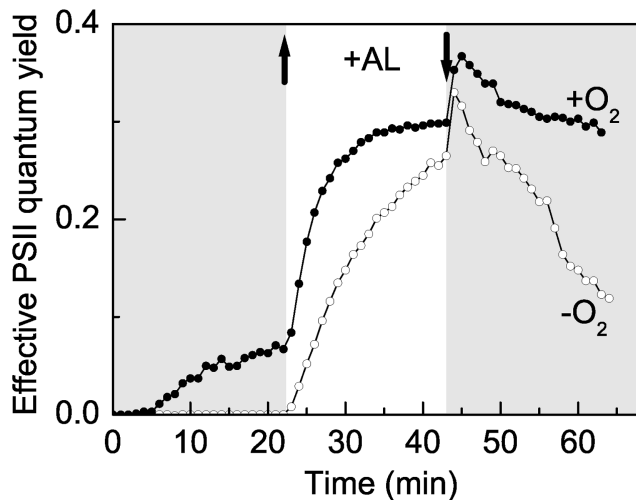


FIG. 6. Effect of molecular oxygen on the time-dependent changes of PSII quantum yield following rehydration of desiccated beachrock samples. Time zero corresponds to the moment at which the desiccated sample was covered with seawater, which previously had been flushed for 5 min either with O_2 (+ O_2) or with N_2 (- O_2). Where indicated, actinic light (AL) was switched on or off. The Y_{640} -parameter is depicted.

ments use very low intensity pulse-modulated measuring light for assessment of the momentary fluorescence yield, F , and the application of brief pulses of saturating light (saturation pulses) for determination of the maximal fluorescence yield, F_m . On the basis of this information, the effective quantum yield of energy conversion in PSII can be calculated (Genty et al. 1989, Schreiber et al. 1994). Because of the low measuring light intensity and the shortness of the saturation pulses, such measurements may be considered nonintrusive (i.e. they do not affect the state of the photosynthetic apparatus). On the other hand, actinic light can cause substantial changes in the state of the photosynthetic apparatus, particularly the redox state of primary acceptors, the first stable acceptor of PSII, which in turn controls the rate of electron transport through PSII. When desiccated beachrock was rehydrated in the presence of actinic illumination, in contrast to dark rehydration the PSII activity (as measured via F_v) increased to high values within 15 min. Hence, there appears to be a light requirement for the recovery of activity. It was the aim of the present study to obtain information on the causes of the observed dark inhibition and light recovery.

By separating the rehydration step from the light-recovery step, it was possible to analyze the kinetics of light recovery. When a rehydrated sample was kept in the dark, the inhibited state could be maintained over extended periods of time and was not affected by the applied weak measuring light and brief pulses of saturating light. Upon onset of actinic light, complex changes of the momentary fluorescence yield (F) and the maximal fluorescence yield (F_m) were induced. In the course of actinic illumination, variable fluores-

cence recovered, thus reflecting an opening of PSII reaction centers. Notably, this recovery primarily involved a decrease of F , whereas F_m remained at a high level. This may be considered unusual, as with most other types of samples, like algal suspensions or leaves, variable fluorescence, $F_v = \Delta F = F_m - F$, is maximal after dark adaptation (where $F = F_o$) and decreases with increasing actinic intensity. This situation results from two major types of deviation from normal behavior, both of which have been reported previously. First, in certain unicellular microalgae, like *S. obliquus*, electron carriers at the acceptor side of PSII can become reduced in the dark, in particular when dark reoxidation by O_2 is prevented under anaerobic conditions (Schreiber and Vidaver 1974, 1975). Second, in contrast to higher plant leaves, cyanobacteria and certain unicellular algae tend to attain the so-called state 2 after dark adaptation (for definition of state 1–state 2, see above), which is characterized by low values of F_m and F_v (Schreiber et al. 1995, Schreiber 1998). Both aspects may be linked, because state transitions are controlled by the redox state of the PQ pool and/or of components of the cyt *b/f* complex (Allen 1992, Allen et al. 1995). Transition to state 2 may be induced in the dark, when the PQ pool is reduced via a thylakoid membrane-bound NADPH-dehydrogenase (Mi et al. 1992, Schreiber et al. 1995). In view of these previous investigations, it appears reasonable to assume that the unusual dark–light–dark fluorescence transients observed with rehydrated beachrock are related to reduction of the PQ pool under anaerobiosis in the dark and subsequent attainment of state 2.

In principle, the inactive state observed after rehydration could also be due to inactivation of the water-splitting complex upon desiccation, the reactivation of which requires light. However, a block at the PSII donor side generally is correlated with quenching of F_m (donor-side dependent quenching), and when this is relieved, the increase of variable fluorescence (and quantum yield) should be paralleled by a rise in F_m and not by a decrease of F , as observed in our experiments. Therefore, although a possible role of water splitting inactivation/reactivation cannot be ruled out, it is not considered further here.

Simultaneous measurements of O_2 concentration and fluorescence gave direct evidence for a decisive role of anaerobiosis. Application of an O_2 microoptode allowed minimally invasive measurements of the O_2 concentration in the surface layer of the beachrock submersed in seawater. Although the water column above the beachrock surface was in equilibrium with air, the surface O_2 concentration dropped to zero in darkness due to the resistance to oxygen mass transfer imposed by the presence of a diffusive boundary layer, in combination with intense oxygen consumption of the beachrock microbial community. (For detailed accounts of diffusive boundary layers, see e.g. Jørgensen and Revsbech [1985] or Boudreau and Jørgensen [2001].) Obviously, after rehydration

the respiratory activity was rapidly restored and the rate of O_2 uptake exceeded the rate of diffusive oxygen supply from the bulk water phase. The high rate of net O_2 uptake was evident from the rapid decline of O_2 concentration after switching the illumination off.

From our combined oxygen and PAM fluorescence measurements, we put forward a model for the action of O_2 on the activity of PSII in the beachrock samples, which is described below. The measured fluorescence signals were dominated by cyanobacteria, particularly when 640-nm excitation was applied. Therefore, the observations must be explained in terms of O_2 effects on cyanobacteria, which have previously only been studied in laboratory strains of *Synechocystis* PCC 6803 (Mi et al. 1992, 2000, Schreiber et al. 1995). In cyanobacteria, the photosynthetic membranes, which may or may not be discrete thylakoid membranes, are characterized by a unique assembly of electron transport components, which on one hand are involved in oxygenic photosynthesis and on the other hand carry out oxidative phosphorylation, with some components being shared by the two processes (Jones and Myers 1963, Peschek and Schmetterer 1982). NADPH-dehydrogenase in cyanobacteria has been suggested to participate in the donation of electrons from respiratory substrates to the photosynthetic electron transport chain (Sandmann and Malkin 1983, Mi et al. 1992). In cyanobacteria, the oxidative pentose phosphate cycle is quantitatively more important than glycolysis in the breakdown of sugars and hence is mainly responsible for the reduction of NADP in the dark (Peschek 1999). Under aerobic conditions in the dark, electrons fed via the NADPH-dehydrogenase into the PQ pool normally end up in the reduction of O_2 , catalyzed by a still unknown oxidase in the so-called process of chlororespiration (Bennoun 1982, Scherer 1990). In the absence of O_2 , the dark reduction of the PQ pool cannot be balanced by the oxidase reaction anymore, and the acceptor side of PSII becomes reduced, with a concomitant increase of fluorescence yield, F , and decrease of the energy conversion efficiency of PSII.

As apparent in Fig. 5, the dark rise of F after the rapid drop after light-off can be accompanied by a pronounced decline of F_m , which is most readily explained by a state 1–state 2 transition. Both the increase in F and the decrease in F_m contribute to the apparent decrease in effective PSII quantum yield. Upon a dark–light transition, PSI oxidizes the PQ pool, but at the same time PQ is also reduced by PSII activity. The steady-state equilibrium redox level is determined mainly by i) the activity of processes on the PSI acceptor side, ii) water-splitting activity, and iii) the distribution of quanta between the two photosystems. Oxygen has an important influence on the PQ redox state upon a dark–light transition, because it serves as the major electron acceptor of PSI before the Calvin cycle is activated and CO_2 becomes the major acceptor (Schreiber and Vidaver 1974, Radmer and Kok 1976). This explains the different responses

of oxygen and fluorescence parameters between the first and second illumination period of Fig. 5. In both cases, the O_2 concentration before illumination was zero, but in the case of the second illumination period the Calvin cycle enzymes were not yet fully dark inactivated, and consequently photosynthetic electron flow could be initiated immediately even in the absence of O_2 upon illumination.

The observed fluorescence changes upon onset of the second illumination point to a pronounced state 2–state 1 transition, a prerequisite for which is the oxidation of the PQ pool by PSI activity (Allen 1992). On the other hand, upon onset of the first illumination, first the system was in state 2 (after being in the dark under anaerobic conditions) and second neither substantial amounts of O_2 nor CO_2 were available as acceptors of PSI. Under these circumstances, it is not surprising that oxygen evolution and photochemical quenching in PSII developed slowly. The limitation at the PSI acceptor side is reflected by the slow rise of F_m ($t_{1/2} \sim 20$ min as compared with $t_{1/2} \sim 1$ min after preillumination), which indicates a slow transition from state 2 to state 1, as the oxidation level of the PQ pool is only slowly increasing.

The pivotal role of O_2 was confirmed by the observation that flushing with O_2 caused an increase of the PSII quantum yield in the dark, suggesting a reoxidation of the PSII acceptor side (i.e. mainly the PQ pool) by O_2 . However, the relatively small increase of the observed quantum yield indicates that the dark-reduction rate was high and could hardly be matched by the diffusive O_2 supply and/or the rate of the oxygenase reaction. Although illumination plays the major role in the restoration of PSII activity, the illumination effect is enhanced by O_2 . As outlined above, it may therefore be assumed that before light activation of CO_2 reduction in the Calvin cycle, O_2 serves as an electron acceptor at the PSI acceptor side. Presumably, it is this O_2 -dependent electron flow, together with cyclic electron flow around PSI, that gives rise to a proton gradient sufficiently high for ATP formation, which is essential for CO_2 reduction. Because O_2 -dependent electron flow as such is associated with zero net O_2 exchange (see e.g. Schreiber et al. 1994), the role of O_2 may be visualized as equivalent to a catalyst in an overall autocatalytic activation process. Before activation of the Calvin cycle, net O_2 evolution can be explained only by electron flow to the relatively small pool of ferredoxin (Fd) and NADP, which are the only electron carriers with sufficiently low redox potentials to stay oxidized under dark anaerobic conditions. Obviously, the involved physiological reactions are rather complex, and it is out of the scope of the present communication to go into more details.

In Figure 7 the three major states of the cyanobacteria photosynthetic apparatus in beachrock are illustrated by highly simplified schemes, which may serve to explain the observed photosynthesis responses toward illumination and O_2 in beachrock. In Fig. 7A, the dark rehydrated state is characterized by anoxic

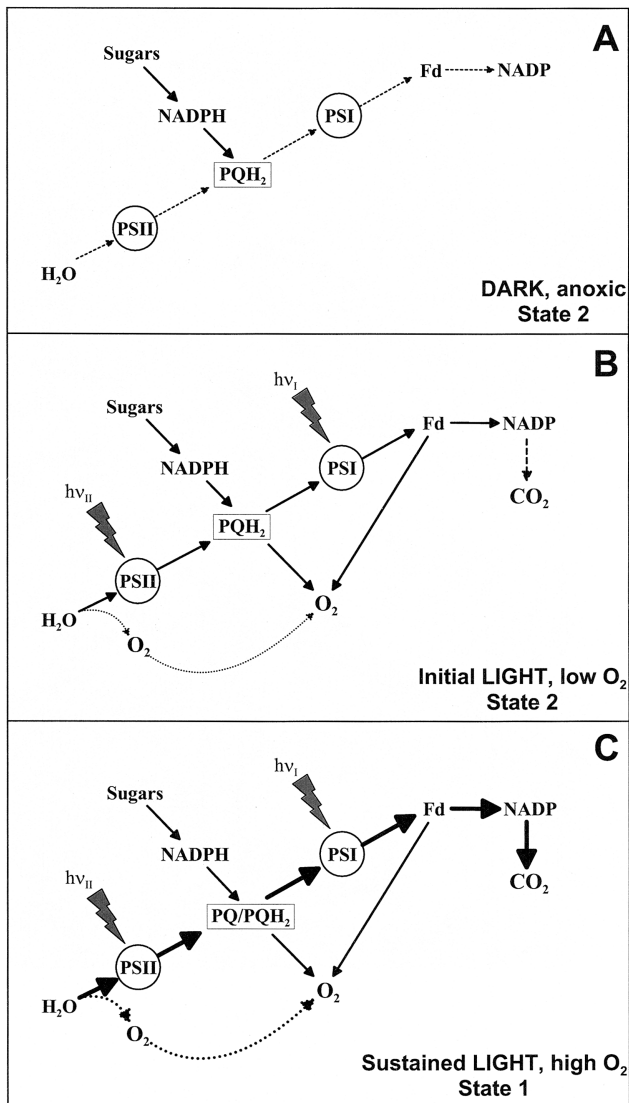


FIG. 7. Schemes characterizing three major states of the cyanobacterial photosynthetic apparatus in beachrock: A. DARK, after rehydration in the dark B. INITIAL LIGHT, briefly (up to a few minutes) after onset of illumination C. SUSTAINED LIGHT, after ca. 10–20 min of illumination. Electron flow is indicated by solid arrows, while oxygen production and diffusion is indicated by dotted arrows. See text for further explanations.

conditions associated with full reduction of the PQ pool and of all other electron carriers, except for Fd and presumably also some NADP. NADPH-dehydrogenase is responsible for keeping the PQ pool fully reduced, with the electrons originally derived from the breakdown of sugars. The system is in pigment state 2, which is characterized by weak excitation of PSII. Immediately after onset of illumination (Fig. 7B), the system is still in state 2, as the PQ pool initially remains highly reduced. Due to PSI driven reduction of the available Fd and NADP, a small amount of PQH₂ becomes oxidized, which immediately is re-reduced by PSII with concomitant evolution of a small amount

of O₂. By diffusion, this O₂ becomes available as electron acceptor at the PSI acceptor side (Mehler reaction) and also at the level of the PQ pool (chlororespiration). These two types of O₂-dependent electron flow may provide ATP required for CO₂ fixation, which will lead to net O₂ evolution, once the Calvin cycle has become light activated, which may be expected within a time range of several minutes. In Fig. 7C a sustained light state is reached after longer illumination. This state is characterized by continuous electron flow to CO₂, the fixation of which is supported by ATP formation associated with O₂-dependent electron flow, which again is enhanced by the increased level of O₂ concentration created by CO₂-dependent electron flow. As the rate of PQH₂ oxidation by PSI and chlororespiration increases, the PQ pool reaches a sufficiently oxidized state for a transition from state 2 to state 1. Hence, eventually a sustained light state is reached that optimizes the photosynthesis rate under given environmental conditions.

This study was carried out as part of the advanced research workshop *Bioreactive surfaces in tropical marine environments*, Heron Island Research Station, February 1–13, 2001. We thank Ove Hoegh-Guldberg and the staff of HIRS for organizing an excellent workshop and for tireless logistic and technical support. Financial support of the Danish Natural Science Research Foundation (to M. K., contract no. 9700549) and of the Australian Research Council (to A. W. D. L. and P. R.) is gratefully acknowledged. Thanks are also due to the Heinz Walz GmbH and Presense GmbH for providing the instrumentation and sensors used in this study.

- Allen, J. F. 1992. Protein phosphorylation in regulation of photosynthesis. *Biochim. Biophys. Acta* 1098:275–335.
- Allen, J. F., Alexciev, K. & Hakansson, G. 1995. Regulation by redox signalling. *Curr. Biol.* 5:869–72.
- Bennoun, P. 1982. Evidence for a respiratory chain in the chloroplast. *Proc. Natl. Acad. Sci. USA* 79:4352–6.
- Bonaventura, C. & Myers, J. 1969. Fluorescence and oxygen evolution from *Chlorella pyrenoidosa*. *Biochim. Biophys. Acta* 189:366–89.
- Boudreau, B. P. & Jørgensen, B. B. [Eds.] 2001. *The Benthic Boundary Layer, Transport Processes and Biogeochemistry*. Oxford University Press, New York, 404 pp.
- Brattström, H. 1992. Marine biological investigations in the Bahamas. Littoral zonation at three Bahamian beachrock localities. *Sarsia* 77:81–109.
- Cribb, A. B. 1966. The algae of Heron Island, Great Barrier Reef, Australia, part 1. A general account. *Univ. Queensland Papers, Gt. Barrier Reef Committee.*, Heron Island Res. Station 1:3–23.
- Davies, P. J. & Kinsey, D.-W. 1973. Organic and inorganic factors in recent beachrock formation, Heron Island, Great Barrier Reef. *J. Sed. Petrol.* 43:59–81.
- Demmig-Adams, B. & Adams, W. W. III. 1992. Photoprotection and other responses of plants to high light stress. *Annu. Rev. Plant Physiol. Plant Mol. Biol.* 43:599–626.
- Genty, B., Briantais, J. M. & Baker, N. 1989. The relationship between the quantum yield of photosynthetic electron transport and quenching of chl fluorescence. *Biochim. Biophys. Acta* 990:87–92.
- Jones, L. W. & Myers, J. 1963. A common link between photosynthesis and respiration in a blue-green alga. *Nature* 199:670–2.
- Jørgensen, B. B. & Revsbech, N. P. 1985. Diffusive boundary layers and the oxygen uptake of sediment and detritus. *Limnol. Oceanogr.* 30:111–22.
- Kautsky, H. & Hirsch, A. 1931. Neue Versuche zur Kohlensäuresassimilation. *Naturwissenschaften* 19:964.
- Klimant, I., Meyer, V. & Köhl, M. 1995. Fiber-optic oxygen mi-

- crossensors, a new tool in aquatic biology. *Limnol. Oceanogr.* 40:1159–65.
- Kolbowski, J. & Schreiber, U. 1995. Computer-controlled phytoplankton analyzer based on 4-wavelengths PAM chlorophyll fluorometer. In Mathis P. [Ed.] *Photosynthesis: from Light to Biosphere*. Vol. V., Kluwer Academic Publishers, Dordrecht, The Netherlands, pp. 825–8.
- Krause, G. H., Briantais, J. M. & Vernet, C. 1982. Photoinduced quenching of chlorophyll fluorescence in intact chloroplasts and algae. Resolution into two components. *Biochim. Biophys. Acta* 679:116–24.
- Krause, G. & Weis, E. 1991. Chlorophyll fluorescence and photosynthesis: the basics. *Annu. Rev. Plant Physiol. Plant Mol. Biol.* 42:313–49.
- Krumbein, W. E. 1979. Photolithotrophic and chemoorganotrophic activity of bacteria and algae as related to beachrock formation and degradation (Gulf of Aqaba, Sinai). *Geomicrobiol. J.* 1:139–203.
- Kühl, M., Glud, R. N., Borum, J., Roberts, R. & Rysgaard, S. 2001. Photosynthetic performance of surface associated algae below sea ice as measured with a pulse amplitude modulated (PAM) fluorometer and O₂ microsensors. *Mar. Ecol. Progr. Ser.* 223:1–14.
- Mi, H., Endo T., Schreiber, U., Ogawa, T. & Asada, K. 1992. Electron donation from cyclic and respiratory flows to photosynthetic intersystem chain is mediated by pyridine nucleotide dehydrogenase in the cyanobacterium *Synechocystis* PCC 6803. *Plant Cell Physiol.* 33:1233–7.
- Mi, H., Klughammer, C. & Schreiber, U. 2000. Light-induced dynamic changes of NADPH-fluorescence in *Synechocystis* PCC 6803 and its *ndhB* defective mutant M55. *Plant Cell Physiol.* 41:1129–35.
- Neumeier, U. 1999. Experimental modelling of beachrock cementation under microbial influence. *Sed. Geol.* 126:35–46.
- Peschek, G. A. 1999. Photosynthesis and respiration of cyanobacteria. In Peschek, G. A., Löffelhardt, W. & Schmetterer, G. [Eds.] *The Phototrophic Prokaryotes*. Kluwer Academic/Plenum Publishers, Dordrecht, The Netherlands, pp. 201–9.
- Peschek, G. A. & Schmetterer, G. 1982. Evidence for plastoquinone-cytochrome *b*/b-563 reductase as a common electron donor to P700 and cytochrome oxidase in cyanobacteria. *Biochem. Biophys. Res. Commun.* 108:1188–95.
- Quick, W. P. & Stitt, M. 1989. An examination of factors contributing to non-photochemical quenching of chlorophyll fluorescence in barley leaves. *Biochim. Biophys. Acta* 977:287–96.
- Radmer, R. J. & Kok, B. 1976. Photoreduction of O₂ primes and replaces CO₂ assimilation. *Plant Physiol.* 58:336–40.
- Sandmann, G. & Malkin, R. 1983. NADH and NADPH as electron donors to respiratory and photosynthetic electron transport in the blue-green alga *Aphanocapsa*. *Biochim. Biophys. Acta* 234: 105–11.
- Scherer, S. 1990. Do photosynthetic and respiratory electron transport chains share redox proteins? *Trends Biochem. Sci.* 15:458–62.
- Schreiber, U. & Vidaver, W. 1974. Chlorophyll fluorescence induction in anaerobic *Scenedesmus obliquus*. *Biochim. Biophys. Acta* 386:97–112.
- Schreiber, U. & Vidaver, W. 1975. Analysis of anaerobic fluorescence decay in *Scenedesmus obliquus*. *Biochim. Biophys. Acta* 386:37–51.
- Schreiber, U., Bilger, W. & Schliwa, U. 1986. Continuous recording of photochemical and non-photochemical chlorophyll fluorescence quenching with a new type of modulation fluorometer. *Photosynth. Res.* 10:51–62.
- Schreiber, U., Bilger, W. & Neubauer, C. 1994. Chlorophyll fluorescence as a non-intrusive indicator for rapid assessment of *in vivo* photosynthesis. *Ecol. Stud.* 100:49–70.
- Schreiber, U., Endo, T., Mi, H. & Asada, K. 1995. Quenching analysis of chlorophyll fluorescence by the saturation pulse method: particular aspects relating to the study of eucaryotic algae and cyanobacteria. *Plant Cell Physiol.* 36:873–82.
- Schreiber, U. 1998. Chlorophyll fluorescence: new instruments for special applications. In Garab, G. [Ed.] *Photosynthesis: Mechanisms and Effects*. Vol. V. Kluwer Academic Publishers, Dordrecht, pp. 4253–8.
- Stephenson, W. & Searles, R. B. 1960. Experimental studies on the ecology of intertidal environments at Heron Island. I. Exclusion of fish from beachrock. *Aust. J. Mar. Freshw. Res.* 11:241–67.
- van Kooten, O. & Snel, J. F. H. 1990. The use of chlorophyll fluorescence nomenclature in plant stress physiology. *Photosynth. Res.* 25:147–50.
- Webb, G. E., Jell, J. S. & Baker, J. C. 1999. Cryptic intertidal microbialites in beachrock, Heron Island, Great Barrier Reef: implications for the origin of microcrystalline beachrock cement. *Sed. Geol.* 126:317–34.
- Williams, W. P. & Allen, J. F. 1987. State 1/state 2 changes in higher plants and algae. *Photosynth. Res.* 13:19–45.